1

2 **Running head**:

3   miRNAs involved in N starvation adaptation

4

5

6

7

8

9

10

11

12

13

14 **Author to whom all correspondence should be sent:**

15 Gang Liang:

16   E-mail: lianggang@xtbg.ac.cn

17 Diqiu Yu

18   E-mail: ydq@xtbg.ac.cn

19 Key Laboratory of Tropical Forest Ecology, Xishuangbanna Tropical Botanical

20 Garden, Chinese Academy of Sciences, Kunming, Yunnan 650223, China.

21 Tel: 86-871-65178133

22 Fax: 86-871-65160916

23

24

25

26

27

28

29

30

31 **Research Area:**

32 Signalling and Response

33

34

35

Two young miRNAs originating from target duplication mediate nitrogen starvation adaptation via regulation of glucosinolate synthesis in *Arabidopsis thaliana*

39

40

41

42

43

44

45

46

One-sentence summary:

Two recently evolved miRNAs enhance plant nitrogen starvation adaptation via regulation of glucosinolate synthesis

50

51

52

53

54

55

56

57

58

Hua He[1,2], Gang Liang[1]*, Yang Li[1,2], Fang Wang[1], and Diqiu Yu[1]*

1 Key Laboratory of Tropical Forest Ecology, Xishuangbanna Tropical Botanical Garden, Chinese Academy of Sciences, Kunming, Yunnan 650223, China.

2 University of Chinese Academy of Sciences, Beijing 100049, China.

64

65

66

67

68

69

70

Footnotes:

75

76

77

Correspondence authors:

Gang Liang:

 E-mail: lianggang@xtbg.ac.cn

Diqiu Yu

 E-mail: ydq@xtbg.ac.cn

83

84

85

86

87

88

89

90

91

92

93

94

95

96

97

98

99

100

101

ABSTRACT

Nitrogen (N) is an essential macronutrient required for plant growth and development. A number of genes respond to N starvation conditions. However, the functions of most of these N-starvation responsive genes are unclear. Our recent survey suggested that many miRNAs are responsive to N starvation in *Arabidopsis thaliana*. Here, we identified a new miRNA (miR5090) from the complementary transcript of the *MIR826* gene. Further investigation uncovered that both miRNA genes recently evolved from the inverse duplication of their common target gene, *AOP2*. Similar to miR826, miR5090 is induced by N starvation. In contrast, the *AOP2* transcript level was negatively correlated with miR826 and miR5090 under N starvation. *GUS*-fused *AOP2* expression suggested that *AOP2* was post-transcriptionally suppressed by miR826 and miR5090. miRNA transgenic plants with significantly low *AOP2* expression accumulated much less methionine-derived glucosinolates, phenocopying the *aop2* mutants. Most glucosinolate synthesis associated genes were repressed under N starvation conditions. Furthermore, miRNA transgenic plants with less glucosinolate displayed enhanced tolerance to N starvation, such as high biomass, more lateral roots, increased chlorophyll and decreased anthocyanin. Meanwhile, N-starvation-responsive genes were upregulated in transgenic plants, implying improved N uptake activity. Our study reveals a mechanism by which *A.thaliana* regulates the synthesis of glucosinolates to adapt to environmental changes in N availability.

INTRODUCTION

miRNAs are a class of endogenous non-coding small RNAs that regulate gene expression post-transcriptionally. miRNAs originate from primary miRNAs (pri-miRNAs) transcribed by RNA polymerase II. Dicer-like proteins in the nucleus orchestrate conversion of the pri-miRNAs to precursor miRNAs (pre-miRNAs) and then to mature miRNAs (Chen X.M., 2005; Voinnet O., 2009). The mature miRNA duplexes are then methylated by HEN1 and exported to the cytoplasm by HASTY (the plant ortholog of exportin 5), where they are incorporated into RNA-induced silencing complexes (RISCs). In the RISC complex, miRNAs can either cleave the target mRNA or repress its translation through perfect, or almost perfect, complementary base pairing with its target sequences (Lu et al., 2008; Voinnet O., 2009).

Plant miRNAs regulate many aspects of plant growth and development, such as leaf morphogenesis (Palatnik et al., 2003), floral development and the juvenile-to-adult transition (Wu et al., 2009). Recent reports revealed that several plant miRNAs are also involved in plant nutrient metabolism (Khraiwesh et al., 2012). Sulfate starvation induces miR395, which regulates sulfate assimilation and allocation by targeting *APSs* (*APS1*, *APS3* and *APS4*) and *SULTR2;1* (*SULFATE TRANSPORTER 2;1*) in *A. thaliana* (Liang et al., 2010). Phosphate deficiency upregulates miR399, which controls phosphate acquisition and root-to-shoot translocation by repressing *PHO2* (*UBC24*) (Chiou et al., 2006). Copper limitation induces miR397, miR398, miR408 and miR857, which regulate copper homeostasis by mediating the cleavage of genes encoding copper/zinc superoxide dismutases, copper chaperone for superoxide dismutase and Laccases (Yamasaki et al., 2007; Abdel-Ghany et al., 2008; Beauclair et al., 2010). During N deficiency, miR169 is downregulated, whereas its targets *NFYA* (Nuclear Factor Y, subunit A) family members are induced. Overexpression of miR169 results in the accumulation of less N than in wild-type, suggesting a role in impairing N uptake (Zhao et al., 2011). In addition, high-throughput sequencing of *Arabidopsis* miRNAs uncovered many miRNAs responsive to different nutrient deficient conditions (Hsieh et al., 2009; Pant et al., 2009; Liang et al., 2012).

Nitrogen (N) is a key component of many fundamental biological molecules,

170   such as nucleic acids, amino acids, proteins and N-containing metabolites.
171   Thus, plants must obtain sufficient N for normal growth and development
172   (Peng et al., 2007; Wang et al., 2012). As sessile organisms, most plants
173   absorb N from the soil through their roots. However, there is not always
174   sufficient N in the soil because soil erosion, rainwater leaching, and microbial
175   consumption have removed it. To cope with this N limitation, plants have
176   evolved sophisticated mechanisms to adapt to inhospitable environments.
177   These adaptation mechanisms include regulating N uptake system activity and
178   modulating root system architecture (Peng et al., 2007; Tsay et al., 2011). N
179   uptake by plant roots involves multiple uptake systems (Vidal et al., 2008;
180   Maathuis, 2009). *Arabidopsis* primarily acquires N in the form of NO_3^- using
181   NO_3^- transporters from the NRT1 and NRT2 families. Some of them are
182   induced by NO_3^- to ensure increased uptake when the substrate becomes
183   available. The plant N status also affects NO_3^- uptake, with glutamine acting as
184   a negative feedback signal (Miller et al., 2007). NH_4^+ is another form of
185   inorganic N that is taken up by a relatively large number of high and low affinity
186   NH_4^+ transporters encoded by the AMT family (Miller et al., 2009). However,
187   the molecular mechanisms of N sensing, the N signaling network and the
188   developmental responses to N limitation are not well studied.

189   Glucosinolates are a group of plant secondary metabolites that are largely
190   limited to species of the order Brassicales, which include nutritionally important
191   *Brassica* crops as well as the model plant *A. thaliana* (Wittstock and Halkier,
192   2002). Glucosinolates are N-rich metabolites; therefore, N availability is crucial
193   for their synthesis. The biosynthesis of glucosinolates includes three main
194   processes: side-chain elongation of amino acids, core structure formation, and
195   modifications of the side-chain (Grubb and Abel, 2006). ALKENYL
196   HYDROXALKYL PRODUCING 2 (AOP2) is responsible for the side chain
197   modification of methionine-derived glucosinolates (Kliebenstein et al., 2001;
198   Grubb and Abel, 2006; Neal et al., 2010). Modifications of the glucosinolate
199   side-chain are particularly important because the structure of the side-chain
200   affects the biological activity of the glucosinolates and their degradation
201   products (Hansen et al., 2007).

202   Although many N-starvation responsive miRNAs have been identified
203   (Krapp et al., 2011; Liang et al., 2012), the functions for most of them are

unclear under N starvation conditions. Our previous research revealed that miR826 is significantly induced by N starvation (Liang et al., 2012). Here, a novel miRNA (miR5090) was identified from the complementary transcripts of *MIR826*. Similar to miR826, miR5090 is also upregulated by N starvation. Further investigation suggested that both miRNAs can improve the adaptation of *A. thaliana* to N starvation by directly affecting the synthesis of methionine-derived glucosinolates.

RESULTS

Identification of a novel miRNA in *A. thaliana*

In our previous work (Liang et al., 2012), we used deep sequencing to analyze two small libraries derived from seedlings with or without N deprivation treatment. We found two small RNAs that completely matched with the complementary transcript (*At4g03038*) of the *MIR826* gene (*At4g03039*) (Fig. 1A). This transcript was annotated as another RNA. By prediction of its RNA secondary structure, a canonical miRNA precursor stem-loop structure was produced. The two small RNAs perfectly correspond to the miRNA/miRNA* complex with 2 nt 3' overhangs (Fig. 1C). We speculated that *At4g03038* is an miRNA-encoding gene. To investigate this hypothesis, we searched the *Arabidopsis* MPSS Plus Database (http://mpss.udel.edu/at) for small RNA signatures that match with the stem loop sequence. We found that many small RNA reads are completely identical to the miR826 and mi826* sequences in the *MIR826* gene, and that many small RNA reads match with the putative miRNA and miRNA* sequence in the *At4g03038* transcript (Fig. 1B; Fig. S1A). The combination of the stem loop structure and putative miRNA/miRNA* sequence suggests that *At4g03038* may be an authentic *MIRNA* gene. To confirm our hypothesis, we cloned the stem loop region downstream of the CaMV 35S promoter, and performed *Agrobacterium*-mediated transient expression experiments in *Nictotiana benthamiana* leaves. The antisense sequence of the putative miRNA was used as a probe to detect the expression of the miRNA by northern blotting. As shown in Fig. S1B, compared with the empty vector with no signal detected, the 35S promoter-driven stem loop

sequence accumulated a high abundance of mature small RNA sequence. To determine whether the small RNA products are DCL1 dependent, we detected their abundance in the *dcl1-9* mutant, revealing that these small RNAs are undetectable in the *dcl1-9* mutant compared with the wild type (Fig. 1D). Analysis of the highthroughput sequencing data deposited in MPSS revealed that both miR826 and the novel miRNA sequences were undetectable in the *dcl1-7* mutant, but highly abundant in the wild type and *dcl2/3/4* mutant (Fig. S1C). Therefore, our results indicate that *At4g03038* is an miRNA-encoding gene. This miRNA was designated as miR5090 according to the miRNA annotation system (Ambros et al., 2003).

MIR826 and MIR5090 are recently evolved miRNAs originating in *A. thaliana* genomes by duplication of *AOP2*

miR826 was identified as a recently evolved miRNA, which is only present in *A. thaliana*. To investigate whether miR5090 is conserved in other plant species, we searched the miRNA database (www.mirbase.org) for potential homologs of miR5090. However, no miR5090 homolog was found. We further searched the NCBI nucleotide database (http://blast.ncbi.nlm.nih.gov) for highly similar sequences of miR5090 by BLASTN, and found that miR5090 only matches with the *A. thaliana AOP2* gene. Thus, the miR5090 sequence is specifically present in *A. thaliana*. When the stem loop region sequence of miR5090 was used in a BLAST search for similar *Arabidopsis* transcripts, the only significant result was *AOP2*, which showed 89% similarity over a region of 278 nucleotides (E-value=$4e^{-52}$) that extends well beyond the 21-nucleotide-long miR5090 pairing site. Target prediction (Dai and Zhao, 2011) results also indicated that *AOP2* is the candidate target of miR5090. Allen et al. (2004) suggested that new miRNAs evolve through inverted duplication of target gene sequences. Therefore, we speculated that the *MIR5090* gene originates from a duplication of its target, *AOP2*. To confirm our hypothesis, we compared the genome sequences of *AOP2* and *MIR5090*. As shown in Fig. 2, six regions (F1 to F6) with a high similarity (>90%) are shared by *AOP2* and *MIR5090*. Apparently, the *MIR5090* gene is a duplicate of the *AOP2* gene 3' terminal region containing two exons and one intron. In contrast to *AOP2*, the *MIR5090*

272 gene contains an extra inverted F5 fragment (Fig. 2), which results in the stem

273 loop structures in miR826 and miR5090 precursors (Fig. 1C). We also

274 compared their flanking sequences with no significant similarity found. In the *A.*

275 *thaliana* chromosome, *MIR826*, *MIR5090*, and three *AOP* genes exist in a

276 cluster (Fig. 2). In contrast, only two *AOP* genes were found in *A. lyrata*, from

277 which *A. thaliana* is thought to be derived (Yogeeswaran et al., 2005). This

278 suggested that *MIR826* and *MIR5090* are recently evolved miRNAs.

279

280 **AOP2 is the common target of miR826 and miR5090**

281

282 The *AOP2* gene has been identified as the target of miR826 (Rajagopalan et

283 al., 2006; Liang et al., 2012), which encodes a 2-oxoglutarate-dependent

284 dioxygenase that is involved in glucosinolate biosynthesis. Interestingly, target

285 prediction results suggested that *AOP*2 is also the target of miR5090. As

286 shown in Fig. 3A, the target site of miR5090 is shifted by 5 nt from that of

287 miR826. Usually, the target cleavage mediated by a plant miRNA occurs in the

288 10th nucleotide from the 5' end of the miRNA (Allen et al., 2005). We identified

289 two *AOP2* cleavage sites by 5'RACE experiment from N-starvation

290 *Arabidopsis* seedlings, both of which are identical to the cleavage sites

291 retrieved from degradome data (German et al., 2008; Liang et al., 2012) and

292 perfectly match with the 10th nucleotides of miR826 and miR5090, respectively

293 (Fig. 3A). Thus, these two cleavage products might result from cleavage by

294 miR826 and miR5090. To further investigate whether both miRNAs mediate

295 the putative cleavage of *AOP2*, we performed an *Agrobacterium*-mediated

296 transient assay by coexpressing the miRNA genes (*35S:MIR826* or

297 *35S:MIR5090*) with *AOP2* (*35S:AOP2*) in *N. benthamiana* leaves. The results

298 showed that *AOP2* mRNA levels decreased to 10% or 30% when

299 coexpressing with miR826 or miR5090 compared with the control level,

300 respectively (Fig. 3C). To further confirm whether the cleavage of *AOP*2 occurs

301 in the predicted target sites, several synonymous substitutions were

302 introduced to generate miR826- and miR5090-resistant versions of *AOP2*

303 (35S:*mAOP2*) (Fig. 3B). When miR826 or miR5090 were coexpressed with

304 *mAOP2,* the mRNA levels of *AOP2* were not affected. These results confirmed

305 that *AOP2* is the common target of miR826 and miR5090.

306

307

The transcript abundance of miR826 and miR5090 is negatively correlated with that of *AOP2* in response to N starvation

310

Previously, we found that miR826 transcript abundance was particularly high in the N deprivation library, and miR5090 transcript was only found in the N deprivation library (Liang et al., 2012). To investigate whether both miRNAs are specifically responsive to N deprivation, we tested the expressions of miR826 and miR5090 in seedlings grown under different nutrient deprivation conditions. In contrast to the slight change caused by sulfur (S), potassium (K), or phosphorus (P) deprivation, both miR826 and miR5090 were strongly induced by N starvation (Fig. 4A), indicating that miR826 and miR5090 were specifically upregulated by N starvation. miRNAs suppress their target transcripts; therefore, the expression of miRNAs is usually inversely correlated with that of their targets. Therefore, we detected the transcript levels of miR826, miR5090 and *AOP2* transcripts in 10-day-old seedlings grown on medium supplemented with different N concentrations (N-sufficient (3 mM), N-low (0.3 mM), and N-free (0 mM)). As expected, both miR826 and miR5090 expression levels increased with the decrease in N concentration, whereas *AOP2* showed the reverse trend (Fig. 4B). Similar results were observed when roots and shoots were examined separately (Fig. S2). These results suggested that *AOP2* expression is negatively correlated with the expressions of miR826 and miR5090.

However, we did not know if the reduction in *AOP2* expression directly resulted from the induction of miRNAs under N-starvation conditions. To uncover the regulation of *AOP2* by miRNAs, we prepared two reporters. First, the wild-type *AOP2* cDNA was fused in frame with a *GUS* gene driven by the 2.9kb genomic region upstream of the start codon of *AOP2* (Fig. 4C). This wild-type reporter (*Pro_{AOP2}:AOP2-GUS*) would allow us to monitor *AOP2* transcriptional and post-transcriptional regulation. In agreement with the qRT-PCR results, *Pro_{AOP2}:AOP2-GUS* was strongly expressed in roots and shoots under N-sufficient conditions, whereas GUS staining was very weak under N-free conditions (Fig. 4C). To reveal the effect of miRNAs on the

expression of *AOP2*, we prepared a second reporter, with mutated *AOP2* (*mAOP2*) (Fig.4C). Compared with N-sufficient conditions, the expression of Pro_{AOP2}:*mAOP2-GUS* was downregulated only moderately under N-free conditions (Fig. 4C). GUS staining in the whole plant indicated that *AOP2* was ubiquitously expressed in inflorescence, silique, cauline and rosette leaves (Fig. 4D). These results demonstrated that under N starvation, the expression of *AOP2* is suppressed by miRNAs at the post-transcriptional level.

Overexpression of miR826 or miR5090 suppresses the accumulation of the *AOP2* transcript

To further understand the functions of miR826 and miR5090, we generated transgenic plants overexpressing miR826 or miR5090. Twelve and eight independent transgenic lines for *35S:MIR826* and *35S:MIR5090* were obtained, respectively. We determined the miRNA expression levels of five independent lines for each genotype. The antisense DNA sequences of the two miRNAs were labeled with ^{32}P and used as probes to detect the expression of these two miRNAs using northern blotting. Compared with the wild-type, all of the transgenic plants we examined produced high quantities of mature miRNAs (Fig. 5A). Further analysis suggested that *AOP2* transcript levels were dramatically downregulated in the transgenic plants (Fig. 5B). When subjected to different N-starvation conditions, the transcript abundance of *AOP2* in transgenic plants remained low compared with the wild-type (Fig. 5B). The overproduction of miR826 or miR5090 correlated well with the decreased *AOP2* mRNA level in transgenic plants, suggesting that miR826 and miR5090 suppress *AOP2* mRNA abundance.

Transgenic plants mimic the phenotypes of *aop2* mutants

The *AOP2* gene displays polymorphism across different *A. thaliana* ecotypes (Kliebenstein et al., 2001). The Cvi ecotype contains a functional *AOP2* gene, whereas Col has a non-functional *AOP2* gene resulting from a 5-bp deletion in its transcript. Therefore, all our experiments are performed in *A. thaliana* Cvi ecotype. Given the significant reduction of *AOP2* in transgenic plants, we

expected that they could mimic the glucosinolate profiles of Col ecotype plants that contain a mutated *aop2*. Thus, we detected the glucosinolate profiles in miR826 and miR5090 transgenic plants to determine whether the composition of the glucosinolates had changed as a result of the downregulation *AOP2* expression. As shown in Fig. 6, Cvi contains AOP2-catalyzed products, 2-propenyl (7.7 min; peak 3) and 3-butenyl (12.2 min; peak 4) glucosinolates. By contrast, Col (a natural *aop2* mutant) accumulated 3-methylsulfinylpropyl (5.2 min; peak 1) and 4-methylsulfinylbutyl (7.0 min; peak 2) glucosinolates, both of which are the substrates of AOP2 (Fig.6). We then detected the glucosinolate profiles of miR826 and miR5090 transgenic plants: high levels of 3-methylsulfinylpropyl and 4-methylsulfinylbutyl glucosinolates, but not AOP2-catalyzed products, were detected. These results suggested that elevated miR826 or miR5090 expression suppresses the function of *AOP2*, resulting in the reduction of methionine-derived glucosinolates.

Altered expression of genes involved in aliphatic glucosinolate synthesis

Glucosinolate biosynthesis involves three stages: (a) chain elongation of selected precursor amino acids (only Met and Phe), (b) formation of the core glucosinolate structure, and (c) secondary modifications of the amino acid side chain (Sønderby et al., 2010). AOP2 is a key regulator for glucosinolate synthesis, which is responsible for the secondary modifications of methionine-derived glucosinolates that are the major components of aliphatic glucosinolates. Considering the downregulation of *AOP2* under N starvation conditions, we asked whether glucosinolate synthesis associated genes would be affected by N starvation. Among the 31 genes (Table 1), 19 of which decreased by 35% in wild type under N-free conditions compared with that under N-sufficient conditions. Under both N-sufficient and N-deficient conditions, the down-regulated genes by N starvation always kept at lower levels in miRNA transgenic plants compared with wild type. It suggested that both N starvation and *AOP2* reduction caused downregulation of glucosinolate synthesis associated genes.

miRNA transgenic plants display enhanced tolerance to N starvation

Considering the fact that miR826 and miR5090 are induced by N starvation, we asked whether they are involved in regulating the adaptation of *A. thaliana* to N deficiency. Under N starvation conditions, plants often show physiological and developmental adaptation, such as small stature, decreased primary root length, increased lateral root density, higher anthocyanin accumulation and lower chlorophyll content (Maathuis 2009; Tsay et al., 2011). Therefore, we evaluated the response of miRNA transgenic plants to N starvation. Wild-type and transgenic plants, which were grown on N-sufficient, N-low, and N-free agar medium, respectively, for 10 days, were used for the analysis. Under N-sufficient and N-low conditions, the fresh weight of transgenic plants was higher than that of the wild-type (Fig. 7A). Although wild-type and transgenic plants displayed similar root systems under N-sufficient conditions, the transgenic plants generated longer primary roots and higher lateral root density than the wild-type under N-low conditions (Fig. 7B, C and Fig. S3). With the reduction of N concentration, all plants produced more anthocyanin. However, under N-sufficient and N-low conditions, the anthocyanin concentration of transgenic plants was lower than in the wild-type (Fig. 7D). In contrast, N starvation resulted in the reduction of chlorophyll concentration in all plants, but under N-sufficient and N-low conditions, more chlorophyll was produced in the transgenic plants compared with the wild-type (Fig. 7E). These results revealed that miRNA transgenic plants display enhanced tolerance to N limitation conditions, although no significant phenotypic difference was observed between the wild-type and transgenic plants under N-free conditions. To determine whether transgenic plants were also tolerant to long-term N starvation, plants were grown on agar medium for three weeks. As shown in Fig.7F, wild-type plants generated more senescent leaves than transgenic plants under N-sufficient conditions. In contrast, under N-low conditions the transgenic plants were significantly bigger than the wild-types, despite similar senescent symptoms. We also determined the phenotypes of plant grown in soil, finding that transgenic plants had a higher growth rate than wild type plants did (Fig. S4). Total N measurement revealed that individual transgenic plant contained more N than individual wild type plant did although their N

442   concentrations were similar in both roots and shoots (Fig. S5).

443

444   **Altered responses to N limitation in transgenic plants**

445

446   To analyze whether the tolerance conferred by the two miRNAs in transgenic

447   plants resulted from variation in N acquisition, we determined the N content of

448   transgenic and wild-types. Five-week-old plants were subjected to N-sufficient

449   and N-free conditions, respectively, for 1 week, and the rosette leaves were

450   used for N concentration analysis. However, no significant difference was

451   observed between the wild-type and transgenic plants (Fig. S4). Considering

452   the high biomass and lateral root density of transgenic plants, we speculated

453   that transgenic plants might facilitate N uptake by the roots. An NO_3^--triggered

454   signaling pathway stimulates elongation of growing lateral roots (Zhang and

455   Forde, 1998). This mechanism involves three genes, *ANR1* (Zhang and Forde,

456   1998), *NRT1.1* and *NRT2.1* (Remans et al., 2006a, b). Expression analysis

457   indicated that these genes were upregulated in transgenic plants under N

458   sufficient conditions (Fig.8A, B). Under N-low conditions, the enhanced lateral

459   root systems (Fig. 7C and Fig. S3) of the transgenic plants correlated well with

460   the elevated expression of *ANR1* (Fig. 8A). NO_3^- and NH_4^+ are the two main

461   forms of N nutrients in soils absorbed by plant roots. NRT2 transporters are

462   responsible for NO_3^- uptake (Miller et al., 2009). Our result revealed that

463   *NRT2.1* expression was increased in transgenic plants under N-sufficient and

464   N-low conditions (Fig. 8C), implying a stimulated N uptake activity. NH_4^+

465   uptake is attributed to AMT-type transporters (Miller et al., 2009). We

466   determined the expressions of *AMT1.1*, *AMT1.2,* and *AMT1.5* (Fig. 8D, E, F),

467   demonstrating that only *AMT1.5* was upregulated in transgenic plants. Taken

468   together, our results suggested that the N uptake system in transgenic plants

469   may be improved, leading to enhanced tolerance to N limitation.

470

471   **DISCUSSION**

472

473   Mineral nutrients are vital to plant growth and thus affect crop yield. Several

474   miRNAs involved in nutrient homeostasis have been characterized, such as

475   miR169 for N (Zhao et al., 2011), miR395 for S (Liang et al., 2010), miR397,

miR398, miR408, and miR857 for Cu (Abdel-Ghany et al., 2008), miR399 for P (Chiou et al., 2006), and miR827 for N and P (Kant et al., 2011). N, one essential macronutrient for plant growth, is often deficient in the environment where plants grow. Our previous research showed that many plant miRNAs are responsive to N starvation, among which miR826 was dramatically induced by N starvation (Liang et al., 2012). Here, we identified a novel miRNA gene (*MIR5090*) from the complementary transcript of *MIR826*. Like miR826, miR5090 was also significantly upregulated by N starvation. Our results revealed that both miR826 and miR5090 regulate *A. thaliana*'s adaptation to low N conditions by affecting glucosinolate synthesis.

MIR826 and _MIR5090_ have recently evolved from their common target, _AOP2_

More than 300 miRNAs were identified in *A. thaliana* (miRbase; www.mirbase.org), about one third of which are conserved across plant species. Generally, a conserved miRNA family contains more than one member. By contrast, there is only one member for miR826 and miR5090 families in *A. thaliana*, implying that they are non-conserved miRNAs. In contrast to conserved miRNAs, miR826 and miR5090 are only identified in *A. thaliana*. We could not find their potential orthologs in *A. lyrata*, which shares over 80% of its miRNA genes with *A. thaliana* (Fahlgren et al., 2010), implying that they are recently evolved miRNAs. To date, two hypotheses for the origins of miRNA have been proposed: one is the inverted duplication of the target (Allen et al., 2004), and the other is random sequence origin (Felippes et al., 2008). The DNA fragment containing the *MIR826* and *MIR5090* genes displays high similarity to the *AOP2* gene (Fig. 2), indicating that they are evolved from an inverted duplication of the *AOP2* sequence. Further sequence analysis revealed that a short DNA fragment (34bp) is inversely duplicated, which contains the stem loop structure of two RNA transcripts (Pri-miR826 and Pri-miR5090). Three *AOP* genes are located in the same chromosome in a tandem manner in Col ecotype (Fig. 2). Ler ecotype contains two *AOP1* genes (*AOP1.1* and *AOP1.2*) and one *AOP3*, but no *AOP2*. Both Col and Cvi contain one *AOP1* gene and one *AOP3* gene (in both ecotypes, *AOP3* is

510 transcriptional silent due to natural variation) (Kliebenstein et al., 2001). Thus,

511 a recent local genome rearrangement event has caused the tandem repeat of

512 *AOP* genes in *A. thaliana*. Over time, mutational drift would lead to erosion of

513 the extended similarities between the originating locus and the inverted repeat.

514 However, the sequences of the *MIR826* and *MIR5090* genes show high

515 similarity to a 3' fragment of the *AOP2* gene, implying that these two miRNAs

516 evolved very recently. A similar example is the *Arabidopsis*-specific young

517 miRNAs, miR161 and miR163, both of which are physically linked to their

518 target loci and retain extended complementarity (Allen et al., 2004). Therefore,

519 *MIR826* and *MIR5090* have recently evolved from the duplication of *AOP2*

520 genomic 3' fragment.

521

522 **AOP2 is downregulated by N-starvation via miR826 and miR5090**

523

524 As a suppressor of target genes, miRNAs often mediate the cleavage of their

525 target transcripts, i.e., regulation occurs at the post-transcriptional level

526 (Voinnet, 2009). Target prediction indicated that *AOP2* is the common target of

527 miR826 and miR5090. Our transient expression experiment revealed that both

528 miRNAs are able to mediate the cleavage of *AOP2* mRNAs. Moreover, the

529 cleavage positions in *AOP2* transcripts perfectly match with the predicted

530 miRNA cleavage sites. When nucleotide mutations were introduced into the

531 miRNA recognition sites, the mutated *AOP2* mRNA became insensitive to

532 miR826 and miR5090, suggesting that sequence complementarity of target

533 sites are crucial for the regulation of *AOP2* by miRNAs.

534 miRNA expression is inversely correlated with the expression of its target,

535 unless that the miRNA and its target are expressed in different tissues or cell

536 compartments (Voinnet, 2009). Upon a decrease in N concentration,

537 expressions of miR826 and miR5090 were upregulated, whereas *AOP2*

538 expression was downregulated. This negative correlation implies that *AOP2*

539 expression is spatio-temporally consistent with its suppressors (miR826 and

540 miR5090). The GUS reporter indicated that *AOP2* is ubiquitously expressed in

541 the whole plant (Fig.4D). GUS expression from the wild-type reporter

542 (*Pro_{AOP2}:GUS-AOP2*) was significantly repressed by N-starvation, whereas

543 that of mutated reporter (*Pro_{AOP2}:GUS-mAOP2*) was less affected by N

544 starvation, indicating *AOP2* is suppressed by miR826 and miR5090 at the
545 post-transcriptional level.

546   The genes from the same family are often targeted by miRNAs from different
547 families. For example, miR160 and miR167 target *ARF* genes (Wang et al.,
548 2005; Yang et al., 2006); miR397, miR408, and miR857 target *Laccase* genes
549 (Abdel-Ghany et al., 2008); and miR168 and miR403 target *AGO* genes (Allen
550 et al., 2005). However, it does not happen frequently that one gene is targeted
551 by more than one miRNA. In *A. thaliana*, the *CHX18* gene is targeted by
552 miR780 and miR856 (Fahlgren et al., 2007). Jeong et al. (2011) demonstrated
553 that miR156a and miR529a target *SPL14* in rice. Our study established that
554 miR826 and miR5090 can target the same target (*AOP2*). These two miRNAs
555 may have different functions under different conditions, because, in addition to
556 N starvation, the expression of *AOP2* is also affected by light and dark (Neal et
557 al., 2010). Alternatively, these two recently evolved miRNAs are currently
558 undergoing evolutionary selection. As revealed by Fahlgren (2007), *MIRNA*
559 genes undergo relatively frequent birth and death, with only a subset being
560 stabilized by integration into regulatory networks.

561

562 **Overexpression of miR826 and miR5090 results in reduced accumulation**
563 **of methionine-derived glucosinolates**

564

565 Our results suggested that *AOP2* is the common target of miR826 and
566 miR5090. Compared with wild-type plants, *AOP2* in miR826 and miR5090
567 transgenic plants is strongly downregulated, regardless of the N status of the
568 environment. Hence, it is expected that transgenic plants can phenocopy *aop2*
569 mutants. AOP2 functions in the side chain modification of methionine-derived
570 glucosinolates (Kliebenstein et al., 2001; Neal et al., 2010). Loss-of-function of
571 *AOP2* led to considerably lower accumulation of methionine-derived
572 glucosinolates than in an *A. thaliana* ecotype with one functional *AOP2* allele
573 (Kliebenstein et al., 2001; Wentzell et al., 2007). Our results also confirmed
574 that *aop2* mutant accumulates much less alkenyl glucosinolates
575 (methionine-derived glucosinolates) (Fig. 6). As expected, miRNA transgenic
576 plants have a very similar glucosinolate profile to *aop2* mutants. Therefore,
577 overexpression of miRNAs is sufficient to reduce the accumulation of

methionine-derived glucosinolates. Our work provides a molecular tool for breeding of *Brassica* vegetable crops with decreased levels of methionine-derived glucosinolates, which has implications for production of functional foods enriched with particular glucosinolates.

Loss-of-function of *AOP2* causes improved N-starvation adaptation in *A. thaliana*

In our N-starvation adaptation experiments, transgenic plants displayed significant growth advantages compared with the wild-type. Corresponding to the phenotypes, the expressions of N-starvation responsive genes were altered in transgenic plants (Fig. 8). The increases in the expressions of N-starvation responsive genes may stimulate N uptake abilities of transgenic plants because the total N amount of individual transgenic plants was higher than that of individual wild type (Fig. S5). Under N-sufficient conditions, no morphological difference was observed for the roots of transgenic plants and wild type. In contrast, the under N-low conditions, transgenic plants had longer primary roots and more lateral roots than wild type. In agreement with root phenotypes, *NRT2.1*, a key regulator in root development under N-limited conditions (Remans et al., 2006b), increased in transgenic plants compared with wild type. Therefore, in addition to the increased expression of N transporters, transgenic plants also enhanced their root systems for adaptation to N-low conditions. Despite having the same origin, the mature sequence of miR826 is different from that of miR5090. However, miR826 transgenic plants displayed phenotypes nearly identical to that of miR5090 transgenic plants. The only common feature for miR826 and miR5090 is that they have the same target gene, *AOP2*. Therefore, loss-of-function of *AOP2* in transgenic plants causes the enhanced adaptation to N starvation. As a key enzyme in glucosinolate synthesis, AOP2 is the major regulator for aliphatic glucosinolate accumulation (Wentzell et al., 2007). An *AOP2* null variant shows up to three-fold less aliphatic glucosinolates compared with the functional *AOP2* variant (Kliebenstein et al., 2001). In miRNA transgenic plants, the function of *AOP2* was dramatically suppressed, which may reduce the consumption of N used for glucosinolate synthesis, thereby increasing the synthesis of

N-containing metabolites that are necessary for plant growth and development under N starvation conditions. Meanwhile, N is one of the major components that are integrated into glucosinolates; therefore, it is possible that the reduction of glucosinolates promotes plants to acquire more N to meet the demand of glucosinolate synthesis. Correspondingly, N starvation also repressed most glucosinolate synthesis associated genes (Table 1). Under N sufficient conditions, the expression levels of glucosinolate synthesis associated genes were lower in miRNA transgenic plants than in wild type, implying that the suppression of *AOP2* by miRNAs mimics N starvation. Indeed, as shown in Fig.8, several N starvation responsive genes were upregulated in miRNA transgenic plants. A similar negative feedback regulation was reported, where N influx increased when glutamine synthesis was blocked (Rawat et al., 1999). Given that the loss-of-function of *AOP2* caused the enhanced N-starvation adaptation, we also compared *mAOP2* transgenic plants with wild type under N-starvation conditions and found that they showed similar N-starvation adaptation (data not shown), which implied that elevated *AOP2* is not sufficient to raise N consumption. Plants have evolved diverse mechanisms to adapt to N starvation conditions. Apparently, reduction of N consumption and increased N absorption is an efficient strategy to maintain normal growth and development of plants when N is unavailable. Our work suggested that *A. thaliana* plants have evolved new miRNAs that affect glucosinolate synthesis, leading to improved adaptation to N starvation conditions.

MATERIALS AND METHODS

Plant Material and Growth Conditions

A. thaliana ecotype-Cape Verde Islands (Cvi) was used as the wild-type plant in all our experiments. The seeds were surface-sterilized with 20% bleach and washed three times with sterile water. Sterilized seeds were suspended in 0.1% agarose and plated on MS medium. After vernalization for 2 days in the dark at 4°C, the plates were transferred to the culture room at 22°C under a 16

645   h light/8 h dark photoperiod. For determination of glucosinolate content,

646   7-day-old seedlings were planted in soil maintained in growth chambers: 22°C

647   and 75% humidity under a 16 h light/8 h dark photoperiod. For observation of

648   root phenotypes, seedlings were grown on vertical MS agar medium

649   containing 0.8% agar. N content in the medium was 3 mM (1 mM NH_4NO_3 and

650   1 mM KNO_3), 0.3 mM (0.1 mM NH_4NO_3 and 0.1 mM KNO_3), and N-free

651   respectively. To evaluate the seed batch variation, homozygous T3 and T4

652   generation transgenic plants were respectively used for evaluation of

653   phenotypes.

654   **5' RACE**

655

656   Following the manufacturer's instructions for the SMARTerTM RACE cDNA

657   Amplification Kit (Clontech), 1μg of total RNA isolated from seedlings grown on

658   N-free MS medium was used for reverse transcription. Gene specific primers

659   (designed according to the protocol) and the UPM primer (provided by kit)

660   were used to conduct PCRs, and purified PCR products were sequenced.

661

662   **Construct Generation**

663

664   The putative promoters of *AOP2* were amplified from A. *thaliana* (Cvi) genomic

665   DNA using primers Pro-AOP2-F and Pro-AOP2-R (Table S1). The fused

666   *Pro$_{AOP2}$-GUS-(m)AOP2* was cloned into the pOCA28 vector containing a

667   kanamycin resistance gene. The genomic sequences containing the

668   stem-loops of MIR826 or MIR5090 were used as synthetic precursor

669   sequences. The sequences were amplified from *A. thaliana* genomic DNA by

670   PCR using primers Pre-miR826-F, Pre-miR826-R, Pre-miR5090-F and

671   Pre-miR5090-R (Table S1). The PCR products of the precursor sequence

672   were cloned into the pMD18-T vector (Takara, http://www.takara.com.cn) and

673   confirmed by sequencing. The miR826 and miR5090 precursors were

674   subcloned into the pOCA30 vector containing the CaMV 35S promoter. All the

675   constructs were then transformed into *Agrobacterium tumefaciens* strain

676   GV3101. *Arabidopsis* transformation was performed by the floral dip method

677 (Clough and Bent, 1998). Transgenic plants were selected using 50 µg/ml
678 kanamycin.

679

680 **Histochemical GUS Staining**

681

682 Plant samples were immersed immediately in 1.5 ml staining solution
683 containing 0.5 mg/ml 5-bromo-4-chloro-3-indoyl-b-D-glucuronide (X-gluc,
684 Sigma) in 0.1 M sodium phosphate buffer (pH 7.3). The reaction was
685 performed in the dark at 37°C until a blue-indigo color appeared. After the
686 reaction, seedlings were rinsed in 0.1 M sodium phosphate buffer (pH 7.3).
687 The samples were then rinsed twice in 70% ethanol to remove chlorophylls.

688

689 **Gene Expression Analysis**

690

691 For gene expression analysis, plants were grown on MS medium with the
692 indicated N concentrations for 10 days.
693   Total RNA was extracted with the Trizol reagent (Invitrogen). Low-molecular
694 weight RNAs were separated by electrophoresis through denaturing 15%
695 polyacrylamide gels, and miRNA gel-blot hybridizations were performed as
696 described previously (Liang et al., 2010). DNA oligonucleotides
697 complementary to miR826 or miR5090 were end-labeled with [α -^{32}P] dATP
698 using T4 polynucleotide kinase and used for hybridizations.
699   For real-time RT-PCR, 0.5 µg of total RNA was reverse transcribed using an
700 oligo(dT)$_{18}$ primer (Fermentas) in a 20 µl reaction mixture with RevertAid
701 M-MuLV reverse transcriptase (Fermentas). After heat inactivation, a 1 µl
702 aliquot was used for real-time quantitative RT-PCR. All quantitative RT-PCR
703 analyses were performed using a Lightcycler FastStart DNA Master SYBR
704 Green I kit on a Roche LightCycler real-time PCR machine
705 (http://www.roche.com), according to the manufacturer's instructions.
706 Real-time RT-PCR for miRNAs was detected by stem-loop RT-PCR. To
707 produce miRNA-fused stem-loop cDNA, 0.5 µg of total RNA was used for the
708 reverse transcription, with miRNA mature-sequence-specific stem-loop RT
709 primers designed according to the stem-loop RT-PCR protocol (Varkonyi-Gasi

710 et al., 2007). *ACTIN2* (*AT3G18780*) was used as a control for quantitative

711 RT-PCR. The primers used in quantitative RT-PCR are listed in Table S1.

712

713

714 **Transient Expression in *N. benthamiana***

715 Constructs were transformed into *A. tumefaciens* strain EHA105 and selected

716 on Luria-Bertani medium containing rifampicin at 50 μg/mL and spectinomycin

717 at 100 mg/L. Agrobacterium cells were then infiltrated into leaves of N.

718 benthamiana. For coinfiltration experiments, equal volumes of an

719 agrobacterium culture containing *35S:MIR826*, *35S:MIR5090*, or vector (OD_{600}

720 = 1.75) and *35S:(m)AOP2* (OD_{600} = 0.25) were mixed before infiltration into *N.*

721 *benthamiana* leaves. Leaves were harvested 3 d after infiltration, and total

722 RNA was extracted for small RNA blotting and real-time RT-PCR experiments.

723

724 **Measurement of Chlorophyll Content**

725

726 Chlorophyll contents were measured as described by Woodward and Bennett

727 (2005). The pigments from leaves of 10-day-old seedlings were extracted with

728 5 ml of dimethylformamide for 24 h in the dark at 4°C, and the optical densities

729 (OD_{664} and OD_{647}) for each sample were measured. The chlorophyll content

730 was calculated as: (($OD_{664} \times 7.04$) + ($OD_{647} \times 20.27$)) $\times 5$ / sample weight (g)

731 =μg chlorophyll /g FW.

732

733 **Measurement of Anthocyanin Content**

734

735 Ten-day-old seedlings grown on MS medium with the indicated N

736 concentrations were used for anthocyanin analysis. Anthocyanin contents

737 were measured as described previously (Rabino and Mancinelli, 1986). The

738 pigments were extracted from leaves with 99:1 methanol:HCl (v/v) overnight at

739 4°C. The OD_{530} and OD_{657} for each sample were measured, and $OD_{530} - 0.25$

740 $\times OD_{657}$ was used to compensate for the contribution of chlorophyll and its

741 products to the absorption at 530 nm.

742

N content Analysis

The shoots and roots of plants grown in soil for four or five weeks were separately harvested and dried at 65°C for 3 d. The samples were milled to a fine powder for N analysis. N analysis was performed using a carbon and nitrogen analyzer (Vario MAX CN; Elementar Analysen systeme GmbH, Germany).

Glucosinolate Extraction

Glucosinolate extraction was performed as described by Kliebenstein (2001) and Neal (2010). Leaves of 5-week-old wild type and transgenic plants were harvested, freeze-dried and then ground to powder. 250 mg of the powder was then suspended in 5 ml of 70% methanol. After incubation at 70°C for 20 minutes, 1ml $Ba(OAc)_2$ (0.4mol/L) was added and centrifuged at 3000 rpm for 5 minutes, and then the supernatant was added to DEAE-Sephadex A25. The column was then washed twice with water and twice with 1 ml of 20 mM sodium acetate. Sulfatase solution (75 μ l) (prepared as described by Graser (2000)) was then added to the column and left to stand overnight. Desulfonated glucosinolates were eluted in 1 ml aliquots of deionised water and analyzed by UPLC-MS/MS.

UPLC-MS/MS Analysis of Glucosinolates

Glucosinolate samples were analyzed using a Waters ACQUITY UPLC system and Xevo™ TQ-S mass spectrometer. Samples (20 μl) were separated using a Agilent zorbax SB-C18 column (4.6× 250 mm i.d., 5 μm particle size) operated at 1 ml/min at 30°C using the following separation gradient described by Neal (2010). Solvent A: H_2O; Solvent B: MeCN: 1.5 - 5% (v/v) B (6 min), 5 - 7% (v/v) B (2 min), 7 - 21% (v/v) B (10 min), 21-29% (v/v) B (5 min), 29 - 57% (v/v) B

773 (14 min), followed by a cleaning cycle: 57 - 93% (v/v) B (2 min), 5 min hold, 93

774 - 1. 5% (v/v) B (3 min), 6 min hold. Eluting compounds were monitored at 229

775 nm. The mass spectral (MS) analysis of glucosinolates was obtained with

776 positive electrospray ionization (ESI) in multiple reaction monitoring (MRM)

777 mode. The ESI source was operated at 4 kV, and the sample cone was

778 operated at 20 V. Nitrogen was used both as bath gas (100°C; 250 L/h) and

779 nebulizing gas (15 L/h). ESI spectra were recorded in the mass range m/z 100

780 -800. Mass spectral of 3-methylsulfinylpropyl, 4-methylsulfinylbutyl, 2-propenyl

781 and 3-butenyl glucosinolates was analyzed with detecting a single M+Na$^+$

782 specific for the glucosinolate being tested. 2-propenyl glucosinolate in the

783 samples was further identified with its standard purchased from Sigma-Aldrich.
784

785 **ACKNOWLEDGEMENTS**
786

789

790 **LITERATURE CITED**

791

792 **Abdel-Ghany SE, Pilon M** (2008) MicroRNA-mediated systemic

793 down-regulation of copper protein expression in response to low copper

794 availability in *Arabidopsis*. J Biol Chem **283:** 15932-15945

795 **Allen E, Xie Z, Gustafson AM, Sung GH, Spatafora JW, Carrington JC**

796 (2004) Evolution of microRNA genes by inverted duplication of target gene

797 sequences in *Arabidopsis thaliana*. Nat Genet **36:**1282-1290

798 **Allen E., Xie Z., Gustafson AM, Carrington JC** (2005) MicroRNA-directed

799 phasing during trans-acting siRNA biogenesis in plants. Cell **121:** 207-221

800 **Ambros V, Bartel B, Bartel DP, Burge CB, Carrington JC, Chen X,**

801 **Dreyfuss G, Eddy SR, Griffiths-Jones S, et al** (2003) A uniform system for

802 microRNA annotation. RNA **9:** 277-279

803 **Beauclair L, Yu A, Bouché N** (2010) microRNA-directed cleavage and
804 translational repression of the copper chaperone for superoxide dismutase
805 mRNA in *Arabidopsis*. Plant J. **62:**454-462

806 **Chen XM** (2005) microRNA biogenesis and function in plants. FEBS Letters
807 **579:** 5923-5931

808 **Chiou TJ, Aung K, Lin SI, Wu CC, Chiang SF, Su CL** (2006) Regulation of
809 phosphate homeostasis by microRNA in *Arabidopsis*. Plant Cell **18:** 412-421

810 **Clough SJ, Bent AF** (1998) Floral dip: a simplified method for
811 *Agrobacterium*-mediated transformation of *Arabidopsis thaliana*. Plant J **16:**
812 735-743

813 **Dai X, Zhao PX** (2011) psRNATarget: A Plant Small RNA Target Analysis
814 Server. Nuc Acids Res **doi:** 10.1093/nar/GKR319

815 **Fahlgren N, Howell MD, Kasschau KD, Chapman EJ, Sullivan CM,**
816 **Cumbie JS, Givan SA, Law TF, Grant SR, Dangl JL, Carrington JC** (2007)
817 High-throughput sequencing of *Arabidopsis* microRNAs: evidence for
818 frequent birth and death of MIRNA genes. PLoS ONE. **2(2):**e219

819 **Fahlgren N, Jogdeo S, Kasschau KD, Sullivan CM, Chapman EJ,**
820 **Laubinger S, Smith LM, Dasenko M, Givan SA, Weigel D, Carrington JC**
821 (2010) MicroRNA gene evolution in *Arabidopsis* lyrata and *Arabidopsis*
822 *thaliana*. Plant Cell **22(4):**1074-1089

823 **Felippes FF, Schneeberger K, Dezulian T, Huson DH, Weigel D** (2008)
824 Evolution of *Arabidopsis thaliana* microRNAs from random sequences. RNA
825 **14:** 2455-2459

826 **German MA, Pillay M, Jeong DH, Hetawal A, Luo S, Janardhanan P,**
827 **Kannan V, Rymarquis LA, Nobuta K, German R, et al** (2008) Global
828 identification of microRNA-target RNA pairs by parallel analysis of RNA ends.
829 Nat Biotech **8:** 941-946

830 **Graser G, Schneider B, Oldham NJ, Gershenzon J** (2000) The methionine
831 chain elongation pathway in the biosynthesis of glucosinolates in Eruca
832 sativa (Brassicaceae). Arch Biochem Biophys **378:** 411-419

833   **Grubb CD, Abel S** (2006) Glucosinolate metabolism and its control. Trends in

834   Plant Sci **11(2):** 89-100

835   **Hansen BG, Kliebenstein DJ, Halkier BA** (2007) Identification of a

836   flavin-monooxygenase as the S-oxygenating enzyme in aliphatic

837   glucosinolate biosynthesis in *Arabidopsis.* Plant J **50:** 902-910

838   **Hsieh LC, Lin SI, Shih AC, Chen JW, Lin WY, Tseng CY, Li WH, Chiou TJ**

839   (2009) Uncovering small RNA-mediated responses to phosphate deficiency

840   in *Arabidopsis* by deep sequencing. Plant Physiol **151(4):** 2120-2132

841   **Jeong DH, Park S, Zhai J, Gurazada SGR, Paoli ED, Meyers BC, Green PJ**

842   (2011) Massive analysis of rice small RNAs: mechanistic implications of

843   regulated microRNAs and variants for differential target RNA cleavage. Plant

844   Cell **23:** 4185-4207

845   **Krapp A, Berthomé R, Orsel M, Mercey-Boutet S, Yu A, Castaings L,**

846   **Elftieh S, Major H, Renou JP, Daniel-Vedele F** (2011) Arabidopsis roots

847   and shoots show distinct temporal adaptation patterns toward nitrogen

848   starvation. Plant Physiol **157:** 1255-1282

849   **Kant S, Peng M, Rothstein SJ** (2011) Genetic regulation by NLA and

850   microRNA827 for maintaining nitrate-dependent phosphate homeostasis in

851   *Arabidopsis.* Plos Genet **7(3):** e1002021

852   **Khraiwesh B, Zhu JK, Zhu JH** (2012) Role of miRNAs and siRNAs in biotic

853   and abiotic stress responses of plants. Biochimica et Biophysica Acta

854   **1819(2):** 137-148

855   **Kliebenstein DJ, Lambrix VM, Reichelt M, Gershenzon J, Mitchell-Olds T**

856   (2001) Gene Duplication in the Diversification of Secondary Metabolism:

857   Tandem 2-Oxoglutarate-Dependent Dioxygenases Control Glucosinolate

858   Biosynthesis in *Arabidopsis.* Plant Cell **13:** 681-693

859   **Liang G, Yang FX, Yu DQ** (2010) MicroRNA395 mediates regulation of sulfate

860   accumulation and allocation in *Arabidopsis thaliana.* Plant J **62:** 1046-1057

861   **Liang G, He H, Yu D** (2012) Identification of nitrogen starvation-responsive

862   microRNAs in *Arabidopsis thaliana.* PLoS ONE **7(11):** e48951

863 **Lu XY, Huang XL** (2008) Plant miRNAs and abiotic stress responses.
864   Biochem Biophys Res Commun **368:** 458-462

865 **Maathuis FJ** (2009) Physiological functions of mineral macronutrients. Curr
866   Opin Plant Biol **12(3):** 250-258

867 **Miller AJ, Fan X, Shen Q, Smith SJ** (2007) Amino acids and nitrate as signals
868   for the regulation of nitrogen acquisition. J Exp Bot **59(1):**111-9.

869 **Miller AJ, Shen Q, Xu G** (2009) Freeways in the plant: transporters for N, P
870   and S and their regulation. Curr Opin Plant Biol **12(3):**284-290

871 **Neal CS, Fredericks DP, Griffiths CA, Neale AD** (2010) The characterisation
872   of AOP2: a gene associated with the biosynthesis of aliphatic alkenyl
873   glucosinolates in *Arabidopsis thaliana*. BMC Plant Biol **10:**170

874 **Palatnik JF, Allen E, Wu XL, Schommer C, Schwab R, CarringtonJC,**
875   **Weigel D** (2003) Control of leaf morphogenesis by microRNAs. Nature
876   **425(6955):** 257-263

877 **Pant BD, Musialak-Lange M, Nuc P, May P, Buhtz A, Kehr J, Walther D,**
878   **Scheible WR** (2009) Identification of nutrient-responsive *Arabidopsis* and
879   rapeseed microRNAs by comprehensive real-time polymerase chain
880   reaction profiling and small RNA sequencing. Plant Physiol **150(3):**
881   1541-1555

882 **Peng MS, Bi YM, Zhu T, Rothstein SJ** (2007) Genome-wide analysis of
883   *Arabidopsis* responsive transcriptome to nitrogen limitation and its regulation
884   by the ubiquitin ligase gene *NLA*. Plant Mol Biol **65:** 775-797

885 **Rabino I, Mancinelli AL** (1986) Light, temperature, and anthocyanin
886   production. Plant Physiol **81:** 922-924

887 **Rajagopalan R, Vaucheret H, Trejo J, Bartel DP** (2006) A diverse and
888   evolutionarily fluid set of microRNAs in *Arabidopsis thaliana*. Genes Dev. **20:**
889   3407-3425

890 **Rawat SR, Silim SN** (1999) AtAMT1 gene expressioin and NH_4^+ uptake in
891   roots of *Arabidopis thaliana*: evidence for regulation by root glutamine levels.
892   Plant J **19:** 143-152

893 **Remans T, Nacry P, Pervent M, Filleur S, Diatloff E, Mounier E, Tillard P,**
894 **Forde BG, Gojon A** (2006a) The *Arabidopsis* NRT1.1 transporter
895 participates in the signalling pathway triggering root colonization of
896 nitrate-rich patches. Proc Natl Acad Sci USA **103:**19206-19211

897 **Remans T, Nacry P, Pervent M, Girin T, Tillard P, Lepetit M, Gojon A** (2006b)
898 A central role for the nitrate transporter NRT2.1 in the integrated
899 morphological and physiological responses of the root system to nitrogen
900 limitation in Arabidopsis. Plant Physiol **140:** 909-921

901 **Sønderby IE, Geu-Flores F, Halkier BA** (2010) Biosynthesis of
902 glucosinolates--gene discovery and beyond. Trends Plant Sci 15: 283-290

903 **Tsay YF, Ho CH, Chen HY, Lin SH** (2011) Integration of nitrogen and
904 potassium signaling. Annu Rev Plant Biol **62:** 207-226

905 **Varkonyi-Gasi, E, Wu R, Wood M, Walton EF, Hellens RP** (2007) Protocol: a
906 highly sensitive RT-PCR method for detection and quantification of
907 microRNAs. Plant Methods **3:**12.

908 **Vidal EA, Gutiérrez RA** (2008) A systems view of nitrogen nutrient and
909 metabolite responses in *Arabidopsis*. Curr Opin Plant Biol **11:** 1-9

910 **Voinnet O** (2009) Origin, Biogenesis, and Activity of Plant MicroRNAs. Cell
911 **136:** 669-687

912 **Wang J, Wang L, Mao Y, Cai W, Xue H, Chen X** (2005) Control of root cap
913 formation by microRNA-targeted auxin response factors in *Arabidopsis*.
914 Plant Cell **17:** 2204-2216

915 **Wang YY, Hsu PK, Tsay YF** (2012) Uptake, allocation and signaling of nitrate.
916 Trends Plant Sci **17(8):**458-467

917 **Wentzell AM, Rowe HC, Hansen BG, Ticconi C, Halkier BA, Kliebenstein**
918 **DJ** (2007) Linking metabolic QTLs with network and cis-eQTLs controlling
919 biosynthetic pathways. PLoS Genet **3(9):** 1687-701

920 **Wittstock U, Halkier BA** (2002) Glucosinolate research in the *Arabidopsis* era.
921 Trends Plant Sci **7:** 263–270

922 **Woodward AJ, Bennett IJ** (2005) The effect of salt stress and abscisic acid

923   on proline production, chlorophyll content and growth of *in vitro* propagated

924   shoots of *Eucalyptus camaldulenis*. Plant Cell Tissue Organ Cult **82:**

925   189-200

926   **Wu G, Park MY, Conway SR, Wang JW, Weigel D, Poethig RS** (2009) The

927   sequential action of miR156 and miR172 regulates developmental timing in

928   *Arabidopsis*. Cell **138:** 750-759

929   **Yang JH, Han SJ, Yoon EY, Lee WS** (2006) 'Evidence of an auxin signal

930   pathway, microRNA167-ARF8-GH3, and its response to exogenous auxin in

931   cultured rice cells'. Nucleic Acids Res, **34:** 1892-1899

932   **Yamasaki H, Abdel-Ghany SE, Cohu CM, Kobayashi Y, Shikanai T, Pilonet**

933   **M** (2007) Regulation of Copper Homeostasis by MicroRNA in *Arabidopsis*. J

934   Biol Chem **282(22):**16369-16378

935   **Yogeeswaran K, Frary A, York TL, Amenta A, Lesser AH, Nasrallah JB,**

936   **Tanksley SD, Nasrallah ME** (2005) Comparative genome analyses of

937   Arabidopsis spp.: inferring chromosomal rearrangement events in the

938   evolutionary history of A. thaliana. Genome Res **15(4):** 505-515

939   **Yuan L, Loqué D, Kojima S, Rauch S, Ishiyama K, Inoue E, Takahashi H,**

940   **von Wirén N** (2007) The organization of high-affinity ammonium uptake in

941   Arabidopsis roots depends on the spatial arrangement and biochemical

942   properties of AMT1-type transporters. Plant Cell **19:** 2636-2652

943   **Zhang H, Forde BG** (1998) An *Arabidopsis* MADS box gene that controls

944   nutrient-induced changes in root architecture. Science **279:** 407-409

945   **Zhao M, Ding H, Zhu JK, Zhang F, Li WX** (2011) Involvement of miR169 in

946   the nitrogen-starvation responses in *Arabidopsis*. New Phytol **190:** 906-915

947 Table 1. Relative expression of genes involved in aliphatic glucosinolate pathway.

		3mM/N-sufficient			0.3mM/N-low			0mM/N-free		
		Wild-type	35S:MIR5090	35S:MIR826	Wild-type	35S:MIR5090	35S:MIR826	Wild-type	35S:MIR5090	3
Side chain elongation										
BCAT3	AT3G49680	1.00	0.97	0.70	0.93	0.76	0.68	0.85	0.78	
BCAT4	AT3G19710	1.00	0.97	0.56	0.80	0.40	0.50	0.32	0.11	
BAT5	AT4G12030	1.00	1.02	0.84	0.93	0.60	0.80	0.50	0.31	
.eu...	AT4G13430	1.00	0.90	0.73	1.25	0.87	0.77	0.90	0.67	
.eu...	AT2G43100	1.00	0.37	0.55	0.79	0.59	0.80	0.47	0.31	
.euL2	AT3G58990	1.00	1.00	0.67	1.06	0.79	0.77	0.61	0.51	
PMLDH1	AT5G14200	1.00	1.02	0.63	0.87	0.61	0.66	0.47	0.36	
PMLDH2	AT1G80560	1.00	0.69	0.69	0.99	1.08	1.21	0.91	0.89	
PMLDH3	AT1G31180	1.00	0.59	0.41	0.91	0.63	0.74	0.62	0.33	

MAM1	AT5G23010	1.00	0.73	0.51	0.68	0.43	0.55	0.60	0.18
MAM3	AT5G23020	1.00	0.13	0.17	0.19	0.14	0.11	0.41	0.16

Core structure

CYP79F1	AT1G16410	1.00	0.91	0.65	0.74	0.56	0.59	0.46	0.17
CYP79F2	AT1G16400	1.00	0.79	0.68	0.98	0.88	0.98	0.74	0.39
CYP83A1	AT4G13770	1.00	0.75	0.53	0.84	0.52	0.47	0.59	0.26
GSTF11	AT3G03190	1.00	0.91	0.79	0.95	0.62	0.77	0.37	0.25
GSTU20	AT1G78370	1.00	0.61	0.44	0.59	0.30	0.37	0.24	0.16
GGP1	AT4G30530	1.00	0.81	0.67	1.19	1.80	1.07	1.63	1.80
SUR1	AT2G20610	1.00	0.68	0.58	1.02	1.17	0.73	0.84	1.06
UGT74C1	AT2G31790	1.00	1.00	0.63	1.10	0.65	0.77	0.70	0.55
ST5b	AT1G74090	1.00	0.94	0.80	1.02	0.83	0.66	0.76	0.72
ST5c	AT1G18590	1.00	0.93	0.56	0.86	0.61	0.61	0.48	0.40

Secondary modification

FMOGX-OX1	AT1G65860	1.00	1.31	0.89	0.86	0.78	0.87	0.84	0.49
FMOGX-OX2	AT1G62540	1.00	1.53	1.08	2.32	1.94	2.95	2.97	2.24
FMOGX-OX3	AT1G62560	1.00	1.02	0.87	0.91	0.68	0.87	0.57	0.24
FMOGX-OX4	AT1G62570	1.00	1.01	0.92	1.98	2.70	2.67	7.37	5.98
FMOGX-OX5	AT1G12140	1.00	1.04	0.88	1.70	1.70	1.88	2.55	2.40
GS-OH	AT4G03060	1.00	0.73	0.81	0.67	0.36	0.26	0.24	0.20
AOP2	AT2G25450	1.00	0.26	0.03	0.50	0.20	0.02	0.31	0.08

Transcription factor

MYB28	AT5G61420	1.00	1.48	1.19	0.78	0.54	0.86	1.00	0.90
MYB29	AT5G07690	1.00	1.09	0.78	0.84	0.59	0.61	0.39	0.19
MYB76	AT5G07700	1.00	0.93	0.80	0.61	0.32	0.36	0.27	0.24

Unkonwn function

AOP1   1.00   0.52   0.21   0.85   0.44   0.20   0.57   0.32

Figure legends

950 **Figure1**. Identification of miR5090.

951 A. Precursor sequences of miR826 and miR5090 with a tally of reads (from the

952 N starvation library) mapping to the hairpins.

953 B. Lines denote the sequences mapping to the miRNA precursors. The

954 thickness and color of the lines correspond to the number of total reads

955 representing each small RNA species in the *Arabidopsis* MPSS Plus Database.

956 C. The predicted miRNA precursors.

957 D. RT-PCR analysis of miRNAs in wild-type and *dcl1-9* mutant.

958

959 **Figure 2**. Extended homology between miRNA genes and the *AOP2* gene,

960 suggestive of common origin. Three *AOP* genes and two miRNA genes are

961 closely linked. The open bars and closed bars indicate introns and extrons.

962 F1-F6 correspond to the homologous sequences between the *AOP2* gene and

963 the miRNA genes.

964

965 **Figure 3**. *AOP2* is the common target of miR826 and miR5090.

966 A. Predicted miRNA/target duplex. Vertical arrows indicate the target cleavage

967 positions. The number indicates the number of corresponding cleavage

968 products from 5'RACE experiment.

969 B. Synonymous nucleotide substitutions in miRNA binding sites of *AOP2*.

970 C. Cleavage of *AOP2* transcripts by miR826 and miR5090 in planta.

971 Constructs harboring the wild-type or mutated *AOP2* driven by the 35S

972 promoter were co-agroinoculated with the *35S:MIR826* or *35S:MIR5090*

973 constructs in tobacco leaves. Empty vector was used as a negative control.

974 Total RNAs were extracted after a 3-d inoculation and examined by qRT-PCR.

975

976 **Figure 4**. *AOP2* is regulated post-transcriptionally.

977 A. Expression of miR826 and miR5090 under different nutrient deficiencies.

978 FN, -N, -P, -S, and -K indicate full nutrient, N, P, S, and K deficiencies.

979 Student's *t* test indicated that the values marked by one asterisk are

980 significantly different from the corresponding wild-type value (P < 0.01; n = 3).

981 B. Expressions of miRNAs and *AOP2* under N starvation. A-B, Ten-day-old

982 seedlings were used for RNA extraction. The quantitative RT-PCR analysis

was repeated for three biological replicates, each of which consisted of three technical replicates. The error bars represent the SDs from triplicate samples.

C. GUS staining under N starvation conditions. The scheme represents two reporters with wild-type or mutated *AOP2.* Ten-day-old seedlings were used for GUS staining.

D. GUS staining under different tissues and organs. 2-month-old *Pro_{AOP2}:AOP2-GUS* reporter line was used for GUS staining.

Figure 5. Expressions of miR826, miR5090, and *AOP2* in wild-type and transgenic plants.

A. Leaves from 4-week-old plants were used for RNA extraction. rRNA/tRNA staining is shown as a loading control. 20μg of total RNA was used for northern blotting. #1-#5 represent different transgenic lines.

B. Expression of *AOP2.* Plants were grown for 10 days on MS medium with the indicated N concentrations. RNA was isolated from whole seedlings. The quantitative RT-PCR analysis was repeated for three biological replicates, each of which consisted of three technical replicates. The error bars represent the SDs from triplicate samples. Student's *t* test indicated that the values marked by one asterisk are significantly different from the corresponding wild-type value (P < 0.01; n = 3).

Figure 6. UPLC profile of glucosinolates from different plants. Peak 1 corresponds to 3-methylsulfinylpropyl glucosinolate. Peak 2 corresponds to 4-methylsulfinylbutyl glucosinolate. Peak 3 corresponds to 2-propenyl glucosinolate. Peak 4 corresponds to 3-butenyl glucosinolate.

Figure 7. Transgenic plants are less sensitive to N starvation.

A. Biomass. Values are the means of three replicates of 20 plants.

B. Primary root length.

C. Lateral root density.

D. Anthocyanin concentration. Shoots were harvested for analysis.

E. Chlorophyll concentration. Shoots were harvested for analysis.

A-E, Ten-day-old plants grown on plates were used for analysis. Error bars indicate the SDs (n = 3). The asterisk indicates statistical significance at P <

1017 0.01 compared with wild-type (Student's *t* test).

1018 F. Three-week-old seedlings grown on medium with the indicated N

1019 concentrations.

1020

1021 **Figure 8**. Expression of N starvation responsive genes.

1022 A. *ANR1*; B. *NRT1.1*; C. *NRT2.1*; D. *AMT1.1*; E. *AMT1.*2; F. *AMT1.5*. A-F,

1023 Roots of 10-day-old plants were used for expression analysis. The quantitative

1024 RT-PCR analysis was repeated for three biological replicates, each of which

1025 consisted of three technical replicates. The error bars represent the SDs from

1026 triplicate samples. Student's *t* test indicated that the values marked by one

1027 asterisk are significantly different from the corresponding wild-type value (P <

1028 0.01; n = 3).

1029

1030 **Supplemental Data**

1031 **Figure S1**. Analysis of small RNA sequences.

1032 A. Precursor sequences of miR826 and miR5090 with a tally of reads mapping

1033 to the hairpins. The numbers represent each small RNA species in the

1034 Arabidopsis MPSS Plus Database (http://mpss.udel.edu/at).

1035 B. Northern blotting of miR5090 mature sequence. *35S:MIR5090* was

1036 transiently expressed in *N. benthamiana* leaves.

1037 C. Read number of miRNA in different genotypes. The small RNA information

1038 was retrieved from Arabidopsis MPSS Plus Database (http://mpss.udel.edu/at)

1039 **Figure S2**. Expression of miRNAs and *AOP2* under N starvation. A-B, Roots

1040 and shoots were harvested separately from 10-day-old seedlings and used for

1041 RNA extraction. The quantitative RT-PCR analysis was repeated for three

1042 biological replicates, each of which consisted of three technical replicates. The

1043 error bars represent the SDs from triplicate samples.

1044 **Figure S3**.Phenotypes of transgenic plants grown on plates.

1045 Ten-day-old seedlings were grown on vertical MS agar medium containing the

1046 indicated N concentrations.

1047 **Figure S4**. Phenotypes of transgenic plants grown in soil.

1048 A. Plants grown in soil for 2, 3, and 4 weeks were photographed.

1049 B. Fresh weight of plants grown in soil for 2, 3, and 4 weeks. Student's *t* test

1050 indicated that the values marked by one asterisk are significantly different from

1051 the corresponding wild-type value (P < 0.01).

1052

1053 **Figure S5**. N contents of wild-type and transgenic plants. Four/five-week-old

1054 plants grown in soil were used for total N measurement.

1055 A. N concentration in roots and shoots.

1056 B. N amount for individual plant. Student's *t* test indicated that the values

1057 marked by one asterisk are significantly different from the corresponding

1058 wild-type value (P < 0.01).

1059

1060 **Table S1**. Primers used in this study.

1061
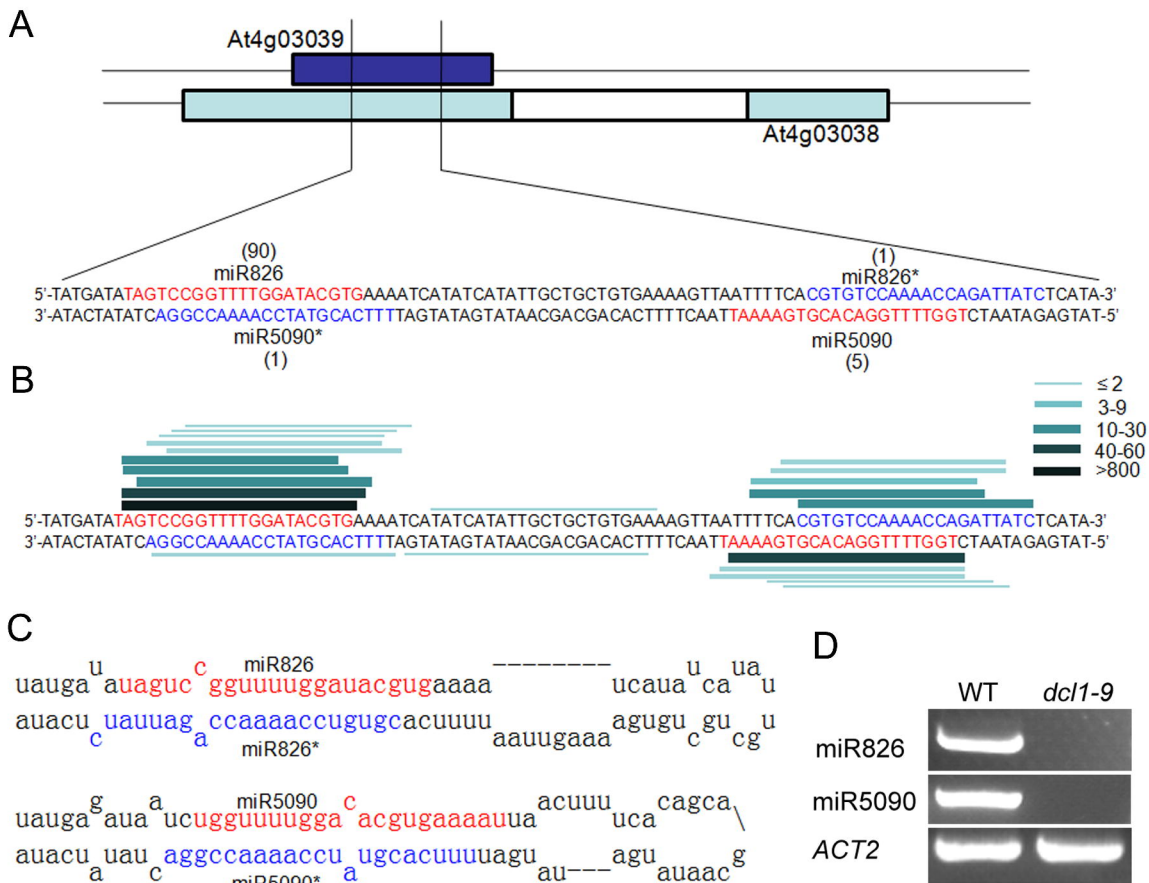
Figure1. Identification of miR5090.

A. Precursor sequences of miR826 and miR5090 with a tally of reads (from the N starvation library) mapping to the hairpins.

B. Lines denote the sequences mapping to the miRNA precursors. The thickness and color of the lines correspond to the number of total reads representing each small RNA species in the Arabidopsis miRSEQ Plus Database.

C. The predicted miRNA precursors.

D. RT-PCR analysis of miRNAs in wild-type and *dcl1-9* mutant
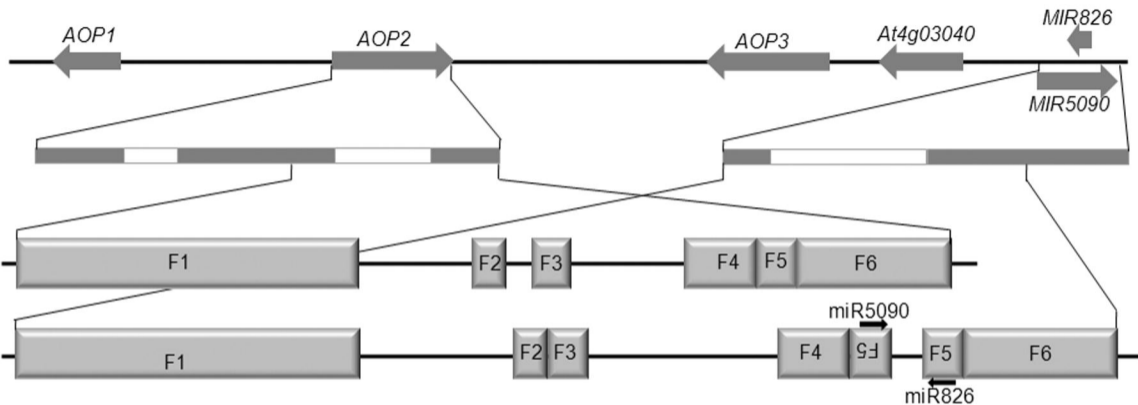
Figure 2. Extended homology between miRNA genes and the AOP2 gene, suggestive of common origin.
Three AOP genes and two miRNA genes are closely linked. The open bars and closed bars indicate introns and extrons. F1-F6 correspond to the homologous sequences between the AOP2 gene and the miRNA genes.
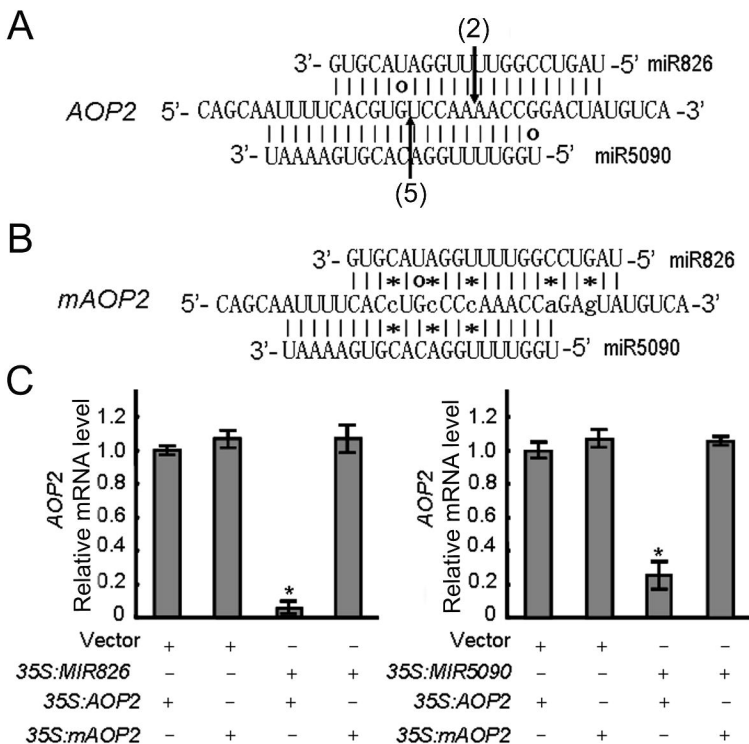
A

(2)

3'– GUGCAUAGGUUUUGGCCUGAU –5' miR826
| | | | |o| | | | | | | | | | | | |
AOP2   5'– CAGCAAUUUUCACGUGUCCAAAACCGGACUAUGUCA –3'
| | | | | | | | | | | | | | | | | | | |o
3'– UAAAAGUGCACAGGUUUUGGU –5'   miR5090

(5)

B

3'– GUGCAUAGGUUUUGGCCUGAU –5' miR826
| | |*|o*| | |*| | | | |*| |*| |
mAOP2   5'– CAGCAAUUUUCACcUGcCCcAAACCaGAgUAUGUCA –3'
| | | | | | | |*| |*| |*| | | | | |
3'– UAAAAGUGCACAGGUUUUGGU –5' miR5090

C

Vector   +   +   –   –   Vector   +   +   –   –
35S:MIR826   –   –   +   +   35S:MIR5090   –   –   +   +
35S:AOP2   +   –   +   –   35S:AOP2   +   –   +   –
35S:mAOP2   –   +   –   +   35S:mAOP2   –   +   –   +

Figure 3. AOP2 is the common target of miR826 and miR5090.

A. Predicted miRNA/target duplex. Vertical arrows indicate the target cleavage positions.

   The number indicates the number of corresponding cleavage products from 5'RACE experiment.

B. Synonymous nucleotide substitutions in miRNA binding sites of AOP2.

C. Cleavage of AOP2 transcripts by miR826 and miR5090 in planta. Constructs harboring the wild-type

   or mutated AOP2 driven by the 35S promoter were co-agroinoculated with the 35S:MIR826 or

   35S:MIR5090 constructs in tobacco leaves.

   Total RNAs were extracted after a 3-d inoculation and examined by qRT-PCR.
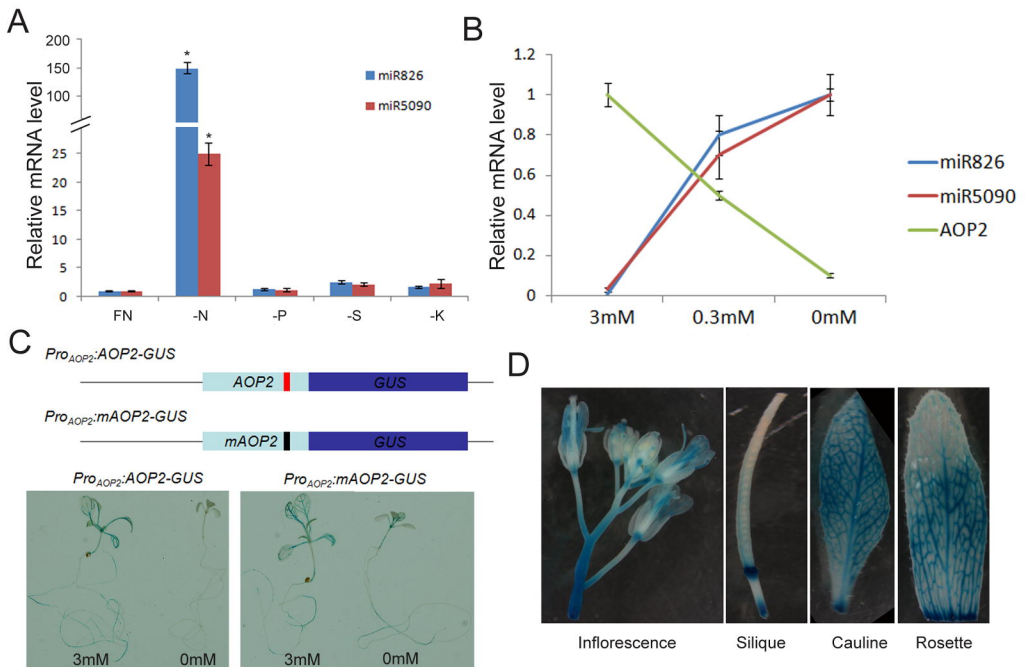
Figure 4. AOP2 is regulated post-transcriptionally.

A. Expression of miR826 and miR5090 under different nutrient deficiencies. FN, -N, -P, -S, and -K indicate
full nutrient, N, P, S, and K deficiencies. Student's t test indicated that the values marked by one asterisk
are significantly different from the corresponding wild-type value (P < 0.01; n = 3).

B. Expressions of miRNAs and AOP2 under N starvation. A-B, Ten-day-old seedlings were used for RNA extraction.
The quantitative RT-PCR analysis was repeated for three biological replicates, each of which consisted of three
technical replicates. The error bars represent the SDs from triplicate samples.

C. GUS staining under N starvation conditions. The scheme represents two reporters with wild-type or mutated
AOP2. Ten-day-old seedlings were used for GUS staining.

D. GUS staining under different tissues and organs. 2-month-old ProAOP2:AOP2-GUS reporter line was used
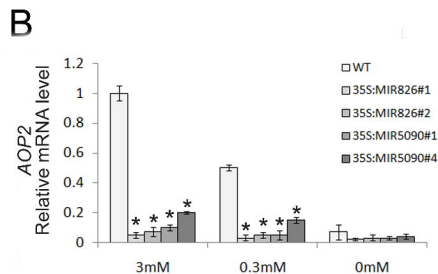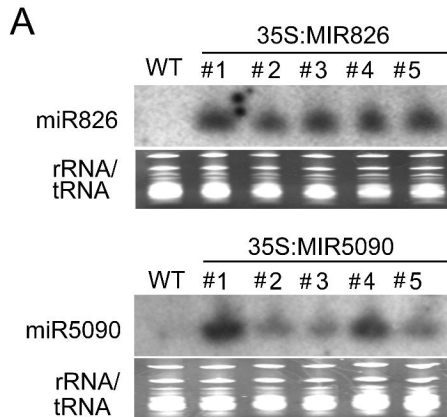for GUS staining.

Figure 5. Expressions of miR826, miR5090, and AOP2 in wild-type and transgenic plants.

A. Leaves from 4-week-old plants were used for RNA extraction. rRNA/tRNA staining is shown as a loading control. 20μg of total RNA was used for northern blotting. #1-#5 represent different transgenic lines.

B. Expression of AOP2. Plants were grown for 10 days on MS medium with the indicated N concentrations. RNA was isolated from whole seedlings. The quantitative RT-PCR analysis was repeated for three biological replicates, each of which consisted of three technical replicates. The error bars represent the SDs from triplicate samples. Student's t test indicated that the values marked by one asterisk are significantly different from the corresponding wild-type value (P < 0.01; n = 3).
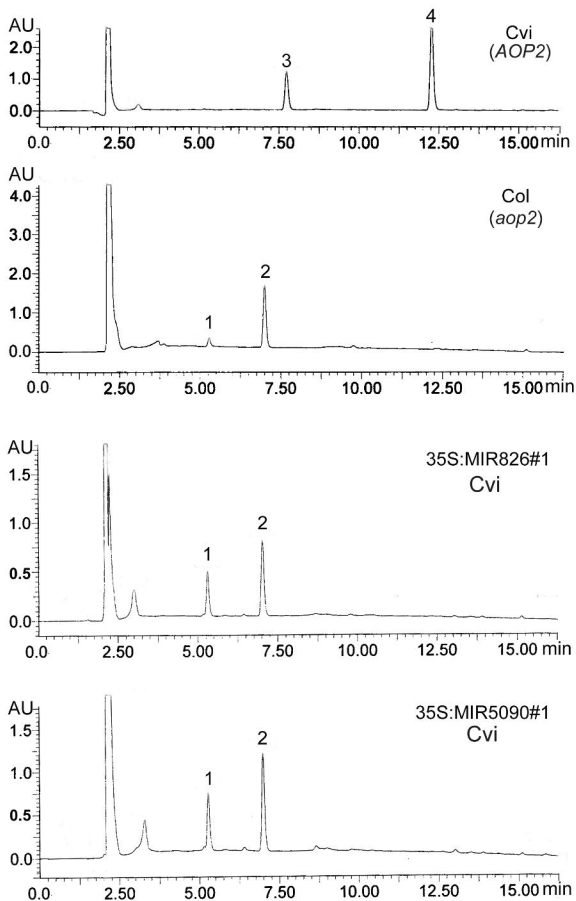
Figure 6. UPLC profile of glucosinolates from different plants.

Peak 1 corresponds to 3-methylsulfinylpropyl glucosinolate.

Peak 2 corresponds to 4-methylsulfinylbutyl glucosinolate.

Peak 3 corresponds to 2-propenyl glucosinolate.
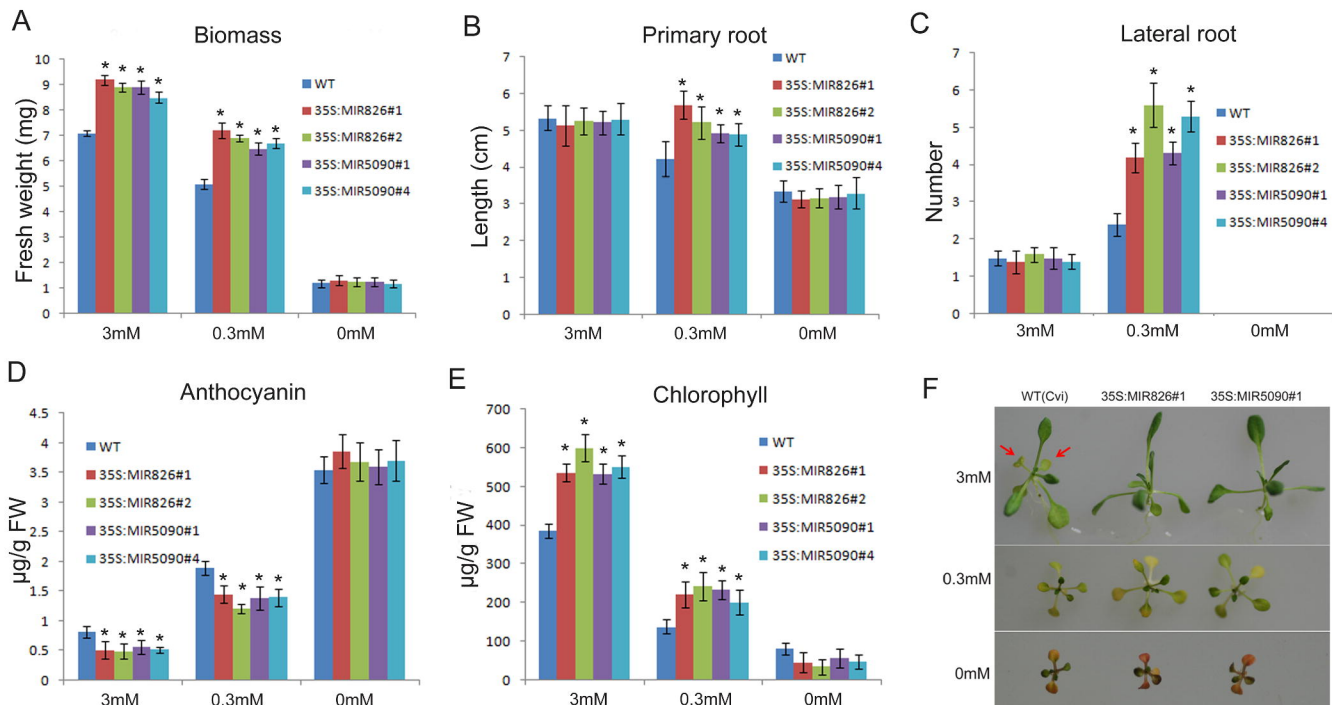
Peak 4 corresponds to 3-butenyl glucosinolate.

Figure 7. Transgenic plants are less sensitive to N starvation.

A. Biomass. Values are the means of three replicates of 20 plants.

B. Primary root length.

C. Lateral root density.

D. Anthocyanin concentration. Shoots were harvested for analysis.

E. Chlorophyll concentration. Shoots were harvested for analysis.

A-E, Ten-day-old plants were used for analysis. Error bars indicate the SDs (n = 3).

The asterisk indicates statistical significance at P < 0.01 compared with wild-type (Student's t-test).

F. Three-week-old seedlings grown on medium with the indicated N concentrations.
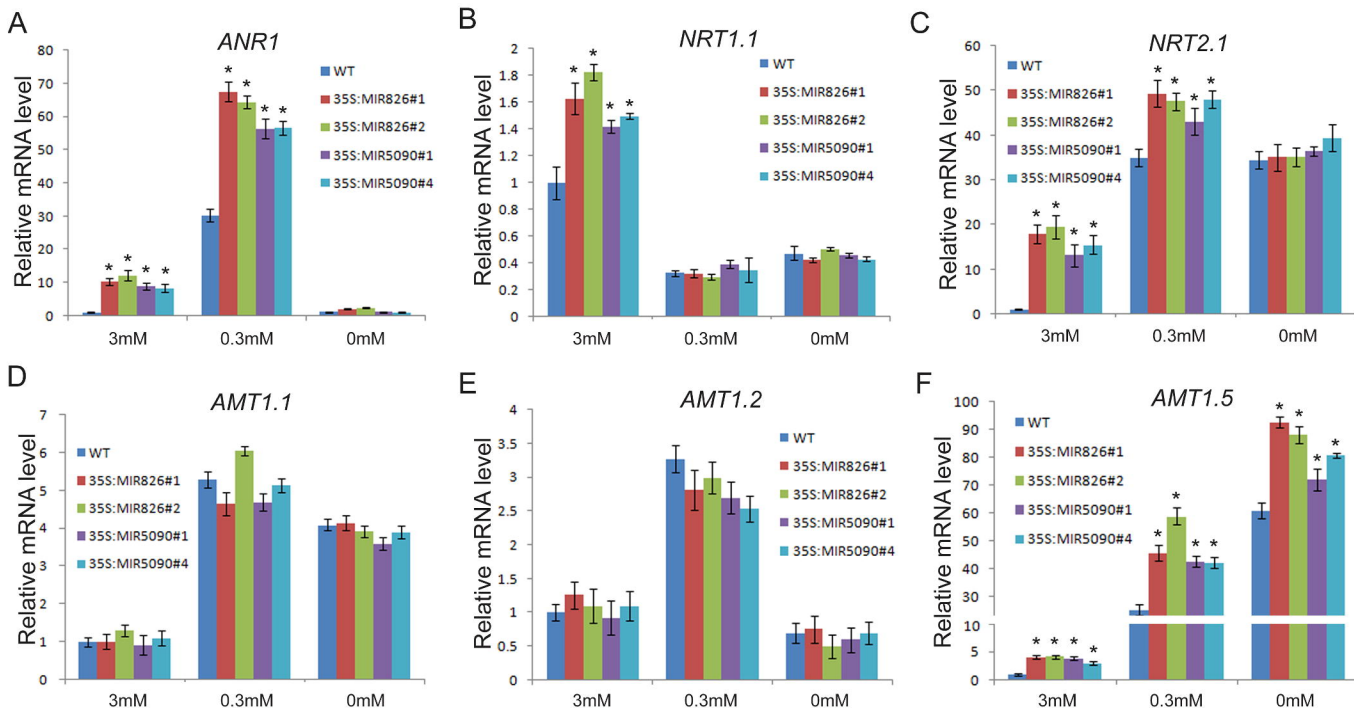
Figure 8. Expression of N-related genes.

A. ANR1; B. NRT1.1; C. NRT2.1; D. AMT1.1; E. AMT1.2; F. AMT1.5.

A-F, Roots of 10-day-old plants were used for expression analysis.

The quantitative RT-PCR analysis was repeated for three biological replicates, each of which consisted of three technical replicates.

The error bars represent the SDs from triplicate samples. Student's t test indicated that the values marked by one asterisk are

significantly different from the corresponding wild-type value (P < 0.01; n = 3).